Research on Engineering Structures & Materials
journal homepage: http://www.jresm.org
MIM Research Group

Research Article

Morpho-structural and compressive mechanical properties of graphene oxide reinforced hydroxyapatite scaffolds for bone tissue applications

Ferzan Fidan[1,a], Naim Aslan[1,2,b*], Mümin Mehmet Koç[3,4,c]

[1]*Department of Strategic Raw Materials and Advanced Technology Applications, Institute of Post Graduate Education, Munzur University, Tunceli, Turkey*
[2]*School of Tunceli, Department of Machinery and Metal Technologies, Munzur University, Tunceli, Turkey*
[3]*School of Medical Service, Department of Medical Service and Techniques Kirklareli University, Kırklareli, Turkey*
[4]*Department of Physics, Faculty of Arts and Sciences, Kırklareli University, Kırklareli, Turkey*

Article Info

Article history:

Received 08 Oct 2022
Revised 04 Dec 2022
Accepted 04 Jan 2023

Keywords:

Hydroxyapatite;
Graphene;
Powder metallurgy;
Space holder;
Mechanical properties

Abstract

Hydroxyapatite (HA) is a unique material that has the potential to be used to replace bones and teeth in the field of orthopedics and dentistry since HA exhibits quite similar biological and chemical characteristics to human bone. Hydroxyapatite ceramics are bioactive materials used to repair damaged human tissue. The pores in the porous hydroxyapatite ceramics provide a mechanical interlock, enabling a solid bond and fixation between the implant and bone. In this study, 0.5wt%, 1wt%, and 1.5wt% graphene oxide (GO) reinforced porous HA structures were obtained using the space-holder method to increase the strength of hydroxyapatite with low mechanical strength. NaCl was used as a spacer, and PEG 400 as a binder. Scaffold structures with 40% porosity rates were sintered at 1000 °C under vacuum. Finally, a compression test was applied to the samples which were previously analyzed by SEM, EDS and XRD. The compressive strengths of 0.5%, 1%, and 1.5% graphene oxide reinforced porous HA samples were determined between 8.04 and 31.14 MPa. The highest compressive strength was recorded as 31.14 MPa in the 1% GO added sample, and the lowest compressive strength was recorded as 8.04 MPa in the 1.5% GO added sample. In addition, it was understood that the mechanical properties did not increase regularly with the increase of graphene oxide reinforcing.

1. Introduction

Scaffold structures are porous structures which were extensively used in tissue engineering applications such as bone repair, cellular infiltration, angiogenesis, nutrient transfer, and disposal of metabolic waste [1]. When tissue is implanted in the body, scaffold structures provide a mechanically stable environment that promotes cell migration, adhesion, and growth because of their interconnected pores [2]. Hydroxyapatite (HA), which is widely used as a bio ceramic, is known as an essential bio ceramic material with chemical and crystallography similarities to the bone matrix [3]. This material is used as the major inorganic component for bones, teeth, and hard tissue restoration and as a bio ceramic implant in orthopedic and dental applications [4, 5]. However, their mechanical properties such as low fracture toughness and low compressive and tensile stress are known to be significant disadvantages [3]. To improve the low mechanical properties of hydroxyapatite, additives such as carbon nano-tube (6), Al_2O_3 [7], ZrO_2, etc. were used as reinforcing material [8]. Among those reinforcing materials, graphene (Gr) and graphene oxide (GO) have recently attracted the attention of researchers because of its unique

*Corresponding author: aslan.naim@gmail.com
[a]orcid.org/0000-0002-1913-2535; [b]orcid.org/0000-0002-1159-1673; [c]corcid.org/0000-0003-4500-0373
DOI: http://dx.doi.org/10.17515/resm2022.546me1008

mechanical, thermal, and electrical properties. GO is an astonishing 2D material which shows astonishing mechanical resistance due to its sp^2 hybrid binding structure. GO is carbon based material; hence, it is non-toxic [9–11]. Gr and GO are also light, flexible, and biocompatible; therefore, it stands out as a promising material in the production of functional bioceramics used in biomedical applications [12]. Mechanical properties and biocompatibility characteristics of Gr and GO-HA composite structures have been reported by several researchers in the literature where different GO additive ratios were evaluated for different scenarios. It was observed that with 0.5wt%, 1wt%, and 1.5wt% GO reinforcing, the elastic modulus and the fracture toughness increased by 86% and 40% (compared to pure HA), respectively; GO addition had also an improving effect on biocompatibility [13, 14].

Powder metallurgy techniques are one of the most common techniques used in the production of porous or scaffold structures due to their low cost and flexibility in combining different components and compounds [15, 16]. Powder metallurgy techniques and space-holder methods are trending methods preferred by researchers for the production of scaffold structures, since such methods provide low processing cost, and high biological activity which enable producers to manufacture materials in desired pore size distribution with well controlled pore shape [16, 17]. NaCl is an affordable material with good biocompatibility and therefore, often preferred as a spacer to obtain scaffold structures. The NaCl keeps its shape under a high pressure, and it can be removed from the structure before sintering via hot water washing [18–20].

Graphene and graphene oxide-reinforced composite structures are a trending topic in the literature; however, investigation of the properties of the HA scaffold structures obtained by the space-holder method in the existence of graphene oxide (GO) has not been discussed. In this study, HA scaffold structures, 0.5wt%, 1wt%, and 1.5wt% GO reinforced HA scaffold structures with 40% porosity were produced by using powder metallurgy and the NaCl spacer hybrid method. The morphological, structural, and mechanical characterizations of the scaffold structures were investigated.

2. Experimental Details

2.1. Production of Scaffold Structures

In this study, hydroxyapatite (<30 μm, Sigma Aldrich) powders were used as a matrix material, and NaCl (100-150 μm, Supelco) particles by volume were used at a rate of 40%. GO, which is used as a reinforcement material, was obtained by the modified hammers method [21]. Graphene reinforcement ratios in GO/HA structures were determined as 0.5wt%, 1wt%, and 1.5wt% by weight.

Firstly, 0.5wt%, 1wt% and 1.5wt% GO powders were added to separate beakers containing 15 ml of distilled water and mixed ultrasonically for 60 minutes. Then, HA powders and GO additives were added to the beakers at determined rates. In order to adjust the pH of the mixture to 7.4, it was mixed with aqueous NaOH buffer solution using a magnetic stirrer for 60 minutes. Then, the mixture was subjected to the ultrasonic homogenizer for 10 minutes. 0.5wt%, 1wt%, and 1.5wt% GO-reinforced HA mixtures were left to dry in an oven at 70 ◦C for 24 h. NaCl space-holder particles were added to the dried GO-reinforced HA powders at a rate of 40% (v/v). In order to ensure the binding of the materials in the mixture, the polymer PEG400 (polyethylene glycol 400) binder was added to the mixture, and the mixture was stirred with a magnetic stirrer. Then, 450 MPa cold press was applied to the unreinforced HA (P40-HA), 0.5wt% (P40-HA/0.5GO), 1wt% (P40-HA/1GO) and 1.5wt% (P40-HA/1.5GO) GO reinforced HA composites, respectively. It should be noted that all samples have 40% porosity which was obtained with NaCl spacer. To dissolve the NaCl particles, which promotes spacing in the pressed HA-based samples,

composite samples were kept in distilled water for 60 minutes. Then, they were placed in an oven at 80 ◦C for 12 hours for the drying process. Finally, the samples were sintered at 1000 ◦C for 1 hour with the help of a vacuum tube furnace (MSE furnace, 1600◦C). The resulting illustrations and producing schematic of the pure HA and HA/GO scaffolds are presented in Figures 1 and 2, respectively.

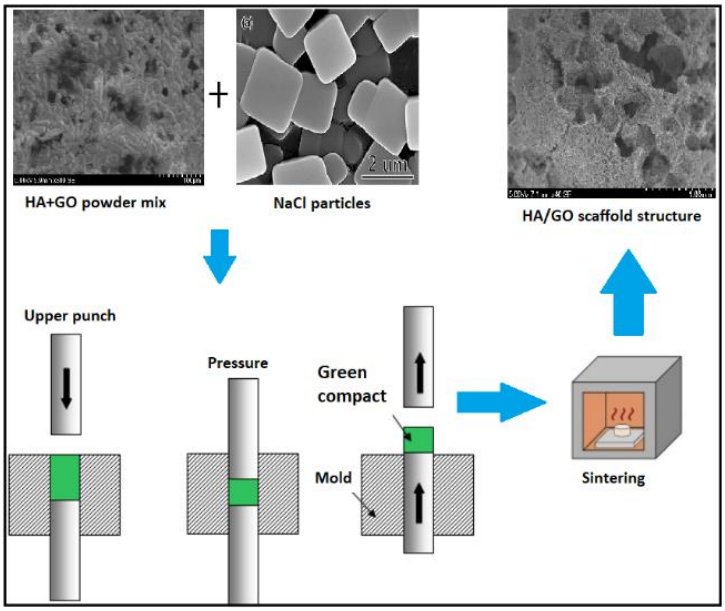

Fig. 1 Production scheme of scaffold structures

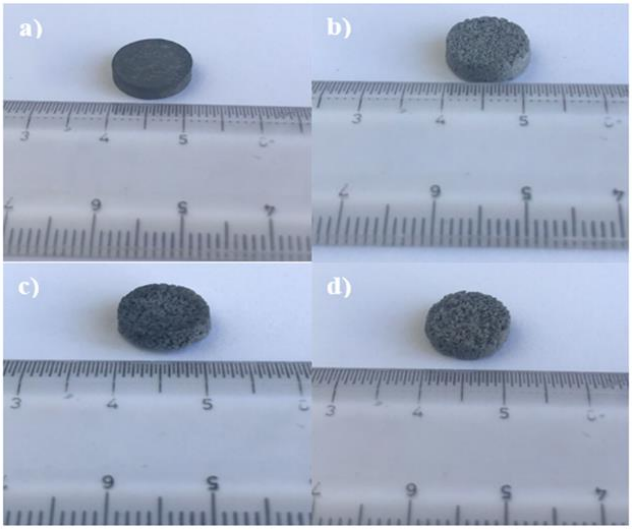

Fig. 2 Images of (a) P40-HA, (b) P40-HA/0.5GO, (c) P40-HA/1GO, (d) P40-HA/1.5GO samples

2.2. Characterization of HA/GO Scaffold Structures

For the structural characterization of the sintered samples, X-ray diffraction analysis (XRD, Rigaku miniflex600) patterns were taken at a scanning speed of 2 degrees/min and in the range of 10-80 degrees. For morphological and elemental analysis, scanning electron microscopy (SEM, Hitachi SU3500) and SEM-dependent energy dispersive X-ray spectroscopy (EDS, Oxford) were used. The tensile device (100 kN, Shimadzu) was used for compression strength. The compression tests were performed on dimensions 10 mm x 6 mm at a speed of 1 $mm.min^{-1}$.

3. Results and Discussion

3.1. Morphological and structural characterizations of scaffold structures

In this study, HA based, 0.5wt%, 1wt%, and 1.5wt% GO reinforced HA-based porous structures were obtained by using 40% NaCl spacers by volume. The SEM-EDS structural images obtained for the HA sample (P40-HA) and shown in Figure 3a. As illustrated in the figure, porous structures and microcracks were observed on the surfaces following the removal of the NaCl spacer. It is believed that microcrack formation is caused by phase separation by the high temperature heat treatment effect on HA. In fact, it is also known that cracks in HA can negatively affect mechanical strength [3]. In addition, the presence of Cl in the EDS spectrum means that NaCl could not entirely be separated from the structure. To prevent the residual NaCl related peak, the NaCl structure should be fully eliminated by keeping the samples in the water for a longer period of time before the sintering process. SEM-EDS analysis of the 0.5% by weight GO reinforced (P40-HA/0.5GO) scaffold sample is shown in Figure 3b. No cracks in the scaffold structures were seen in the SEM images. The pores in the scaffold structures were found to be relatively smaller. No volumetric shrinkage in samples was observed. As expected, no carbon peak was observed in the P40-HA sample without GO additive in the EDS spectrum, while a significant carbon peak was observed in the GO-reinforceed scaffold structures. Therefore, the presence of the carbon (C) peak in the EDS may be an indication of the GO additive. It is also seen that the peak C is 15% by weight. Such a strong C related peak may also be attributed to the PEG debris which may be stuck to the free GO radicals on the surface of scaffold structures. The SEM images and EDS spectrum of the 1 wt% reinforced GO (P40-HA/1GO) structures are shown in Figure 3c. The SEM image showed a morphological structure with random pores and no cracks. Furthermore, the presence of C in the EDS spectrum almost doubled in comparison to the P40-HA/0.5GO. The presence of Cl was also observed in the P40-HA/1GO scaffold structure.

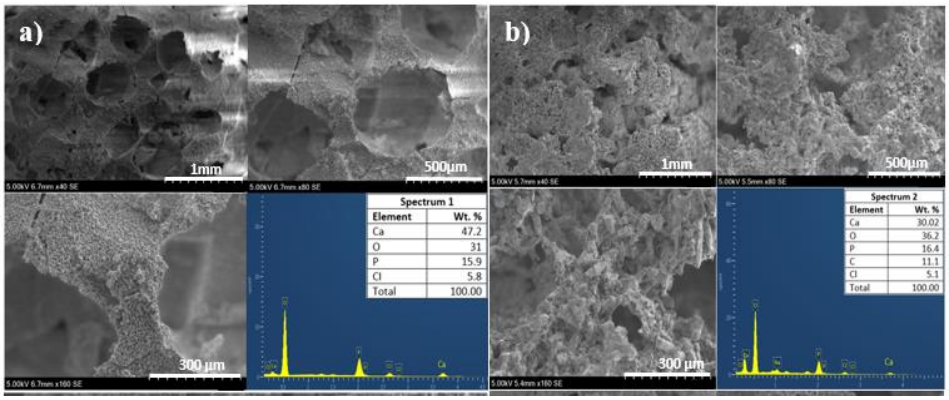

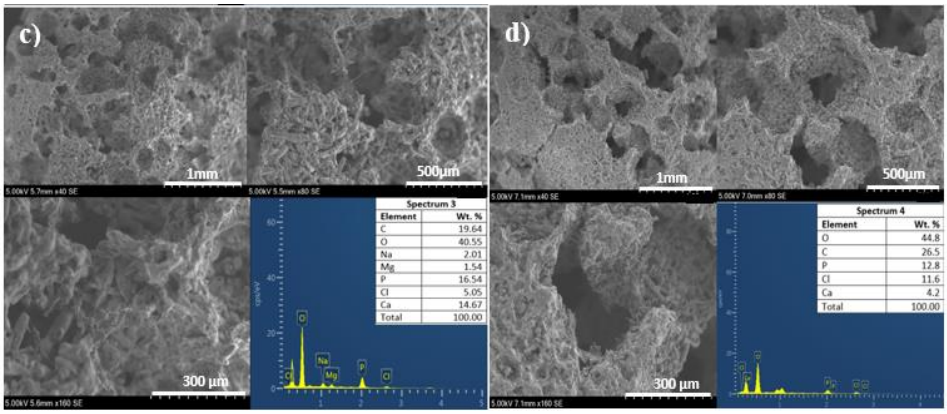

Fig. 3 SEM images and EDS spectra of (a) P40-HA, (b) P40-HA/0.5GO, (c) P40-HA/1GO, (d) P40-HA/1.5GO structures

The SEM images and EDS spectrum of the P40-HA/1.5GO sample reinforced with 1.5 wt% GO are presented in Figure 3d. P40-HA/1.5GO scaffold showed slightly different morphology than those of the P40-HA/0.5GO and P40-HA/1GO structures, as well as the presence of dimensional reduction and crack-forming pores. Overall surface and active sites seemed to be more homogeneous and uniform. It can be attributed to the fact that the GO additive can be formed after 1wt% with its high coefficient of expansion and strong binding of apatite forms to itself [12]. It is believed that the dosage of GO additive can be a limiting entity and can create a disadvantage when higher levels of additive are achieved.

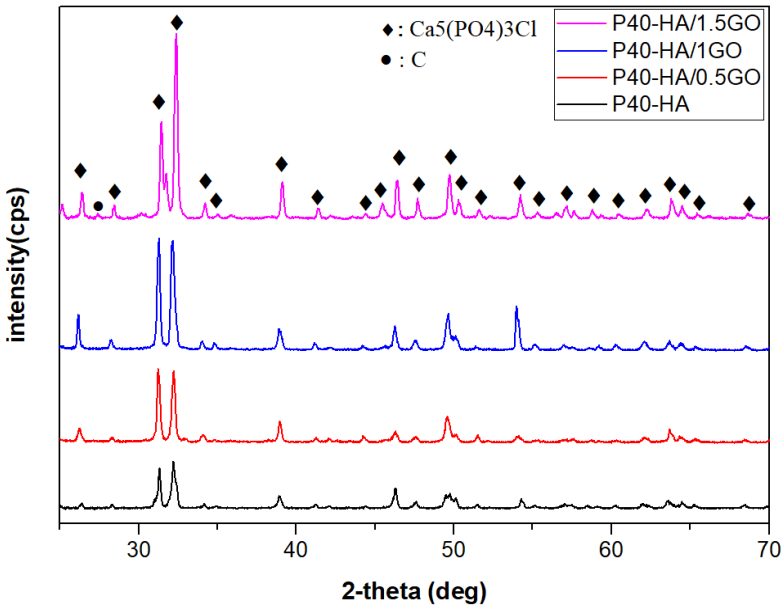

Fig. 4 XRD analysis results of P40-HA, P40-HA/0.5GO, P40-HA/1GO and P40-HA/1.5GO samples

X-ray diffraction patterns were used to determine the elemental analysis of the pore structures obtained. The XRD spectra of P40-HA, P40-HA/0.5GO, P40-HA/1GO, and P40-HA/1.5GO samples by weight are given in Figure 4. As shown in the figure, characteristic peaks of chlorapatite due to heat treatment were observed. In addition, it was observed that the C peak occurred as a result of GO reinforcement. The presence of carbon peak became more apparent with the rise of GO reinforcement. Again, Tricalcium phosphate (TCP) and $CaHPO_4$ structures, which can be formed due to heat treatment [10,12], were not found in porous structures. The sharp peaks formed by both HA and GO reinforced HA porous structures can be explained by the presence of crystallinity of these structures. After sintering, the characteristic peaks became more pronounced with the removal of water and moisture from the structures.

3.2. Mechanical Measurements

The compression test was applied to the P40-HA, P40-HA/0.5GO, P40-HA/1GO, and P40-HA/1.5GO scaffold structures and the force-elongation values were obtained. The stress-strain curves and compressive strength graphs derived from these force-elongation values are given in Figure 5. The compressive strength of the P40-HA, P40-HA/0.5GO, P40-HA/1GO, and P40-HA/1.5GO scaffolds were measured as 24.6, 28.4, 31.14, and 8.04 MPa, respectively. It is found that there is an increase in mechanical strength with 0.5wt% GO reinforcement and it achieves the highest level in 1wt% GO reinforcement. However, there was a significant reduction in the mechanical strength for 1.5wt% GO reinforcement. This can be attributed to HA cracks in the scaffold structure and supports our claim that surface cracks increase with the GO reinforcement in Figure 3. Furthermore, it is considered that the addition of GO with sp^2 hybrid bond structure increases the coefficient of expansion, thus tending to bind more to HA and increase cracks [12]. As a matter of fact, the increase in the amount of GO in the matrix material HA (especially over 1wt%) makes it possible to create cracks and negatively affect the mechanical properties due to the fact that the very strong carbon bonds form a tighter bond with the HA forms together with the heat treatment [10, 21].

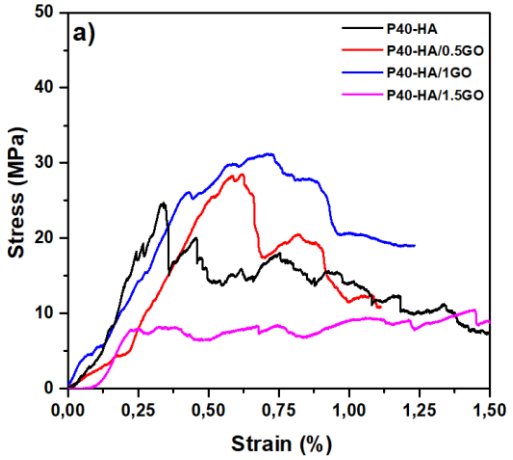

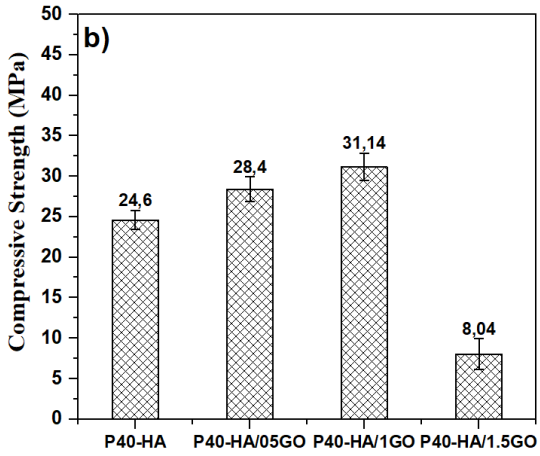

Fig. 5. (a) stress-strain curve and (b) compressive strength values of P40-HA, P40-HA/0.5GO, P40-HA/1GO and P40-HA/1.5GO samples

There are various studies in the literature to improve the mechanical strength of HA composite structures. Gr nanoplatlet-nHA composites with various reinforcing ratios were produced by Kumar et al. While the resulting compression strength values were 87 MPa in the undoped HA structure, the highest compression strength value was measured as 96 MPa in the 0.5wt% Gr nanoplates reinforced HA composite structure [23]. In another study, as a result of the compressive strength test applied to PEEK/HA composite structures with different ratios of GO, the lowest value was measured as 45 MPa in the 0.25% GO reinforcing sample, while the highest value was measured as 65.41 MPa in the 1% GO composite structure [24]. Due to the high pores of the obtained scaffold structures, it is possible that the mechanical values of these scaffold structures are lower than Gr/GO-reinforced HA composites.

4. Conclusion

In our study, we used GO as a reinforcement material to enhance the mechanical properties of the HA scaffolds. Unreinforced HA scaffold, 0.5 wt%, 1wt%, and 1.5wt% GO reinforced HA scaffold structures were obtained by powder metallurgy and 40% (v/v) NaCl spacers. The morpho-structural and mechanical properties of the unreinforced HA scaffolds, 0.5wt%, 1wt%, and 1.5wt% GO reinforced HA scaffold structures were investigated. As a result of the morpho-structural characterizations, it was observed that the cracks on the surface increased with the increase of GO additive and the rate of cracks was slightly higher in the 1.5wt% GO added sample. It was observed that the carbon contents of the HA scaffold structures with 0.5%, 1% and 1.5% GO by weight were higher than the amount of additives in the EDS spectrum. This may be because some residues remain on the scaffold structures in the tube furnace when the polymer binder is removed by vacuum heat treatment. As a result of the XRD analysis, chlorapatite peaks were prominently formed in the structure due to the heat treatment and the C peak was observed due to the GO contribution. In both EDS and XRD analysis, in order to minimize the presence of CI in apatite forms, the NaCl particles in HA can be dissolved in water before heat treatment and completely removed. Stress-strain curves of porous P40-HA structures with 0.5 wt%, 1 wt% and 1.5 wt% GO additives by weight were given and the compression strength values obtained from these curves were calculated. The compressive strengths of the 40% porous HA-GO composite structures were measured between 8.04 and 31.14 MPa. The highest compressive strength was obtained with 31.14 MPa in the 1wt% GO added sample, while

the lowest value was measured as 8.04 MPa in the 1.5wt% GO added sample. Our results were compared with the previous results which was similar to our works. It was seen that our results were coherent with the previously published reports where GO was used as reinforcement material in HA scaffolds. Our results suggest that GO-HA scaffold structures can be a potential candidate for cancellous bone tissue implant applications.

References

[1] Feng C, Zhang K, He R, Ding G, Xia M, Jin X, et al. Additive manufacturing of hydroxyapatite bioceramic scaffolds: Dispersion, digital light processing, sintering, mechanical properties, and biocompatibility. J Adv Ceram 2020 93. 2020 Jun 5 [cited 2022 May 30];9(3):360-73. https://doi.org/10.1007/s40145-020-0375-8

[2] Baino F, Novajra G, Vitale-Brovarone C. Bioceramics and scaffolds: A winning combination for tissue engineering. Front Bioeng Biotechnol. 2015;3:202. https://doi.org/10.3389/fbioe.2015.00202

[3] Zhou H, Lee J. Nanoscale hydroxyapatite particles for bone tissue engineering. Acta Biomater. 2011 Jul 1;7(7):2769-81. https://doi.org/10.1016/j.actbio.2011.03.019

[4] Prakash C, Singh G, Singh S, Linda WL, Zheng HY, Ramakrishna S, et al. Mechanical Reliability and In Vitro Bioactivity of 3D-Printed Porous Polylactic Acid-Hydroxyapatite Scaffold. J Mater Eng Perform. 2021 Jul 1 [cited 2022 Apr 30];30(7):4946-56. https://doi.org/10.1007/s11665-021-05566-x

[5] Senthilkumaran CK, Sugapriya S. Hydroxyapatite Formation on the Antase Phasetitanium Dioxide Nanoparticles. Proceedings of the First International Conference on Combinatorial and Optimization, ICCAP 2021, https://doi.org/10.4108/eai.7-12-2021.2314715

[6] Balani K, Zhang T, Karakoti A, Li WZ, Seal S, Agarwal A. In situ carbon nanotube reinforcements in a plasma-sprayed aluminum oxide nanocomposite coating. Acta Mater. 2008 Feb 1;56(3):571-9. https://doi.org/10.1016/j.actamat.2007.10.038

[7] Tercero JE, Namin S, Lahiri D, Balani K, Tsoukias N, Agarwal A. Effect of carbon nanotube and aluminum oxide addition on plasma-sprayed hydroxyapatite coating's mechanical properties and biocompatibility. Mater Sci Eng C. 2009 Aug 31 [cited 2022 Jul 10];7(29):2195-202. https://doi.org/10.1016/j.msec.2009.05.001

[8] Lahiri D, Singh V, Keshri AK, Seal S, Agarwal A. Carbon nanotube toughened hydroxyapatite by spark plasma sintering: Microstructural evolution and multiscale tribological properties. Carbon N Y. 2010 Sep 1;48(11):3103-20. https://doi.org/10.1016/j.carbon.2010.04.047

[9] Silva M, Alves NM, Paiva MC. Graphene-polymer nanocomposites for biomedical applications. Polym Adv Technol. 2018 Feb 1 [cited 2022 Nov 25];29(2):687-700. https://doi.org/10.1002/pat.4164

[10] Aslan N, Aksakal B, Dikici B, Sinirlioglu ZA. Graphene reinforced hybrid-bioceramic coatings on porous-Ti6Al4V for biomedical applications: morphology, corrosion resistance, and cell viability. J Mater Sci. 2022 Sep 1 [cited 2022 Nov 25];57(35):16858-74. https://doi.org/10.1007/s10853-022-07695-7

[11] Eivazzadeh-Keihan R, Alimirzaloo F, Aghamirza Moghim Aliabadi H, Bahojb Noruzi E, Akbarzadeh AR, Maleki A, et al. Functionalized graphene oxide nanosheets with folic acid and silk fibroin as a novel nanobiocomposite for biomedical applications. Sci Rep. 2022 Dec 1 [cited 2022 Nov 25];12(1). https://doi.org/10.1038/s41598-022-10212-0

[12] Aslan N, Aksakal B. Effect of graphene reinforcement on hybrid bioceramic coating deposited on the produced porous Ti64 alloys. J Porous Mater. 2021 Aug 1 [cited 2022 Apr 30];28(4):1301-13. https://doi.org/10.1007/s10934-021-01081-5

[13] Zhang L, Liu W, Yue C, Zhang T, Li P, Xing Z, et al. A tough graphene nanosheet/hydroxyapatite composite with improved in vitro biocompatibility. Carbon N Y. 2013 Sep 1;61:105-15. https://doi.org/10.1016/j.carbon.2013.04.074

[14] Baradaran S, Moghaddam E, Basirun WJ, Mehrali M, Sookhakian M, Hamdi M, et al. Mechanical properties and biomedical applications of a nanotube hydroxyapatite-reduced graphene oxide composite. Carbon N Y. 2014 Apr;69:32-45. https://doi.org/10.1016/j.carbon.2013.11.054

[15] Choy MT, Tang CY, Chen L, Wong CT, Tsui CP. In vitro and in vivo performance of bioactive Ti6Al4V/TiC/HA implants fabricated by a rapid microwave sintering technique. Mater Sci Eng C. 2014 Sep 1;42:746-56. https://doi.org/10.1016/j.msec.2014.06.015

[16] Aslan N, Aksakal B, Findik F. Fabrication of porous-Ti6Al4V alloy by using hot pressing technique and Mg space holder for hard-tissue biomedical applications. J Mater Sci Mater Med. 2021 Jul 1 [cited 2022 Apr 30];32(7):1-11. https://doi.org/10.1007/s10856-021-06546-2

[17] Topuz M, Dikici B, Gavgali M. Titanium-based composite scaffolds reinforced with hydroxyapatite-zirconia: Production, mechanical and in-vitro characterization. J Mech Behav Biomed Mater. 2021 Jun 1;118:104480. https://doi.org/10.1016/j.jmbbm.2021.104480

[18] Ye B, Dunand DC. Titanium foams produced by solid-state replication of NaCl powders. Mater Sci Eng A. 2010 Dec 15;528(2):691-7. https://doi.org/10.1016/j.msea.2010.09.054

[19] Jha N, Mondal DP, Dutta Majumdar J, Badkul A, Jha AK, Khare AK. Highly porous open cell Ti-foam using NaCl as temporary space holder through powder metallurgy route. Mater Des. 2013 May 1;47:810-9. https://doi.org/10.1016/j.matdes.2013.01.005

[20] Topuz M, Dikici B, Gavgali M, Yilmazer Y. Effect of hydroxyapatite:zirconia volume fraction ratio on mechanical and corrosive properties of Ti-matrix composite scaffolds. Trans Nonferrous Met Soc China. 2022 Mar 1 [cited 2022 Apr 30];32(3):882-94. https://doi.org/10.1016/S1003-6326(22)65840-0

[21] Hummers WS, Offeman RE. Preparation of Graphitic Oxide. J Am Chem Soc. 1958 Mar 1;80(6):1339. https://doi.org/10.1021/ja01539a017

[22] Liu Y, Huang J, Li H. Synthesis of hydroxyapatite-reduced graphite oxide nanocomposites for biomedical applications: Oriented nucleation and epitaxial growth of hydroxyapatite. J Mater Chem B. 2013 Apr 7;1(13):1826-34. https://doi.org/10.1039/c3tb00531c

[23] Kumar S, Gautam C, Mishra VK, Chauhan BS, Srikrishna S, Yadav RS, et al. Fabrication of Graphene Nanoplatelet-Incorporated Porous Hydroxyapatite Composites: Improved Mechanical and in Vivo Imaging Performances for Emerging Biomedical Applications. ACS Omega. 2019 Apr 24;4(4):7448-58. https://doi.org/10.1021/acsomega.8b03473

[24] Peng S, Feng P, Wu P, Huang W, Yang Y, Guo W, et al. Graphene oxide as an interface phase between polyetheretherketone and hydroxyapatite for tissue engineering scaffolds. Sci Reports 2017 71. 2017 Apr 20 [cited 2022 Sep 1];7(1):1-14. https://doi.org/10.1038/srep46604